CMS Physics Analysis Summary

Contact: cms-pag-conveners-heavyions@cern.ch 2024/10/08

Evidence of the medium response to hard probes with Z-hadron correlations in PbPb and pp collisions at $\sqrt{s_{\mathrm{NN}}} = 5.02$ TeV

The CMS Collaboration

Abstract

The first measurement of low transverse momentum (p_{T}) charged hadron pseudorapidity and azimuthal angle distributions relative to Z bosons in PbPb collisions at nucleon-nucleon center-of-mass energy $\sqrt{s_{\mathrm{NN}}} = 5.02$ TeV is presented. This study utilizes PbPb collision data recorded in 2018 with an integrated luminosity of $1.67 \pm 0.03\,\mathrm{nb}^{-1}$, as well as pp collision data acquired in 2017 with an integrated luminosity of $301 \pm 6\,\mathrm{pb}^{-1}$. For the first time in PbPb collisions, the azimuthal angle and pseudorapidity distributions of charged hadrons relative to Z bosons are measured in bins of charged hadron p_{T} to search for in-medium parton shower modifications and medium recoil effects. The analysis focuses on events containing at least one Z boson with $40 < p_{\mathrm{T}} < 350$ GeV. A significant modification in the azimuthal angle and pseudorapidity distributions for charged hadrons in the low p_{T} range, around 1 to 2 GeV, is observed compared to reference measurements from pp collisions. The results are consistent with expectations from phenomenological models, including medium recoil and the medium response to hard probes traversing the quark-gluon plasma. The data provide significant new information about the correlation between hard and soft particles in heavy ion collisions, which can be used to test predictions of various jet quenching models. In data comparisons with models, the first evidence for medium recoil and hole effects caused by a hard probe is found.

Quantum chromodynamics (QCD) predicts that a state known as the quark-gluon plasma (QGP), which consists of deconfined quarks and gluons, is formed at high temperatures and high density [1, 2]. The QGP, consisting of deconfined quarks and gluons, is created in relativistic heavy ion collisions [3] and has been the focus of high-energy nuclear physics experiments at RHIC [4–7] and the LHC [8, 9]. Parton scatterings with high momentum transfer occur much earlier than the formation of the QGP. Thus, such partons can serve as tomographic probes of the plasma [10]. These partons strongly interact with the QGP and lose energy through interacting with the medium, an effect which results in "jet quenching." Experimental measurements of high-transverse-momentum (p_{T}) hadrons [11–16] and jets [17–23] formed by the fragmentation of high-momentum partons have provided evidence establishing the jet quenching phenomenon. However, the details of the jet quenching mechanism remain elusive. Processes such as collisional energy loss, where partons lose energy through interactions with medium constituents, and medium-induced radiation in perturbative QCD-based models, slow down the parton as it traverses the QGP. In AdS/CFT-based models, a drag force, scaled to account for the differences between QCD and infinitely colored charge field theory, similarly reduces the parton's energy when passing through the medium [24]. Additionally, medium recoils and the response induced by hard probes can contribute to producing low transverse momentum particles associated with the high-energy parton (see recent reviews in Refs. [25, 26]). Since both contributions are associated with the temperature scale of the order of hundreds of MeV, separating them using their transverse momentum distributions is difficult. This highlights the need for more experimental efforts to separate different contributions to the jet quenching mechanism and to determine the relevance of medium recoils and medium response.

Unlike strongly interacting particles, electroweak bosons do not significantly interact with the QGP [27–31]. Therefore, measurements of jets produced in the same hard scattering as these bosons offer a controlled configuration for the initial hard scattering [32–35]. The p_{T} of the electroweak boson reflects the initial energy of the associated parton before any energy loss occurs due to interactions with the medium [36, 37]. Among the electroweak bosons, Z bosons, through their muon decay products, offer the cleanest hard-scattering scale tags in the CMS experiment for Z+jet events [35, 38]. This advantage stems from the fact that unlike isolated photons, which require a complex isolation procedure that could introduce measurement biases on particle production around the photon candidate, identifying Z bosons is straightforward. In particular, the Z boson signal, reconstructed via their dimuon decay channel, has minimal background contamination. The non-Z boson background in the dimuon channel is found to be negligible [39]. Capitalizing on the high quality Z boson reconstruction provided by the CMS detector, this work explores the presence of a diffusion wake trailing the outgoing partons on the opposite side of the Z boson. The experiment facilitates the study of medium response and recoil in a phase space far away from the outgoing parton [40–42] by looking at the charged hadron spectra around the Z boson. Moreover, examining the angular distributions of hadron particles relative to the Z boson, sorted by bins of hadron particle p_{T}, allows us to scan the phase space to determine where the medium response and recoil effects are most significant. Finally, at high charged-hadron p_{T}, we search for the large-angle scattering between medium to high p_{T} partons and QGP constituents [43, 44].

This note presents the first measurement of the Z-hadron two-particle correlation function in bins of hadron transverse momentum. Charged hadron spectra tagged by Z bosons are studied as a function of azimuthal angle difference between the Z boson and the charged hadron ($\Delta\phi_{\mathrm{ch,Z}} \equiv \phi^{\mathrm{Z}} - \phi^{\mathrm{trk}}$) and their rapidity difference ($\Delta y_{\mathrm{ch,Z}} \equiv y^{\mathrm{Z}} - \eta^{\mathrm{ch}}$). This study utilizes PbPb collision data at nucleon-nucleon center-of-mass energy $\sqrt{s_{\mathrm{NN}}} = 5.02$ recorded in 2018 with an integrated luminosity of 1.67 ± 0.03 nb^{-1}, as well as pp collision data acquired in 2017 with

an integrated luminosity of 301 ± 6 pb^{-1} at the same energy. The Z bosons selected for the analysis have transverse momenta within the $40 < p_{\mathrm{T}}^{\mathrm{Z}} < 350$ GeV range, while the charged hadrons must have transverse momenta ($p_{\mathrm{T}}^{\mathrm{ch}}$) greater than 1 GeV. In events with more than one Z boson, the highest p_{T} boson is used for the correlation analysis.

The central feature of the CMS detector [45] is a superconducting solenoid of 6 m internal diameter, providing a magnetic field of 3.8 T. Within the solenoid volume are a silicon pixel and strip tracker, a lead tungstate crystal electromagnetic calorimeter (ECAL), and a brass and scintillator hadron calorimeter. Hadron forward (HF) calorimeters extend the pseudorapidity coverage up to $|\eta| = 5.2$. For PbPb events, the HF signals are used to determine the degree of overlap ("centrality") of the two colliding nuclei [17]. Muons are measured in gas-ionization detectors located outside the solenoid.

The Z boson event samples are selected online using dedicated lepton triggers [46]. The triggers on $Z \to \mu^+\mu^-$ events require one muon with $p_{\mathrm{T}} > 12$ GeV and $|\eta| < 2.4$ [46]. Noncollision events are removed in the offline analysis following the procedure in Ref. [16]. The average pileup, defined as the mean number of additional collisions within the same bunch crossing, is 2 in pp collisions and negligible in PbPb collisions. In the pp analysis, events with a single primary vertex are selected to reject events with pileup. The centrality measurement is based on percentiles of the distributions of total energy deposited in the HF calorimeters, representing the fraction of the total inelastic hadronic cross-section, starting at 0% for the most central collisions [17]. The results for PbPb collisions are presented in three centrality intervals: 0–30%, 30–50%, and 50–90%.

The PYTHIA 8.212 [47] Monte Carlo (MC) event generator, tuned with the underlying event (UE) tune CP5 [48], and MADGRAPH5_aMC@NLO [49] next-to-leading order (NLO) program (interfaced with PYTHIA), are used to simulate Z+jet signal events. In the case of PbPb collisions, embedded samples are created by embedding PYTHIA MADGRAPH5_aMC@NLO signal events in minimum bias (MB) heavy ion events modeled using the HYDJET 1.9 MC event generator [50]. These events are then propagated through the CMS apparatus using the GEANT4 toolkit [51], and are used to evaluate reconstruction and selection efficiencies and calibrations and to study the background.

The muon selection requires reconstructed track segments in at least two muon detector planes and a good-quality fit when connecting them to tracker segments [52]. For both pp and PbPb data, muons must have $p_{\mathrm{T}} > 20$ GeV and fall within the acceptance of the muon detectors, $|\eta| < 2.4$. The charged hadron track reconstruction used in both pp and PbPb collisions is described in Ref. [53]. Corrections for tracking efficiency, detector acceptance, and misreconstruction rate are obtained following the procedure outlined in Ref. [16]. The selection criteria are identical with those described in Ref. [16] for the pp and PbPb data.

The Z boson candidates are identified using an oppositely charged muon pair, with a reconstructed invariant mass in the interval 60–120 GeV and $40 < p_{\mathrm{T}}^{\mathrm{Z}} < 350$ GeV. About 2000 events pass these selection criteria. Muon pairs are corrected for losses due to detector acceptance, reconstruction efficiency, muon identification, and trigger selections [52]. Each Z boson candidate is correlated with all tracks in the same event that pass the $p_{\mathrm{T}}^{\mathrm{ch}} > 1$ GeV and $|\eta^{\mathrm{ch}}| < 2.4$ selections. To avoid including the tracks of the Z boson candidate decay products, each track used in the correlations is required to fall outside a cone radius (defined as $\sqrt{(\Delta\eta)^2 + (\Delta\phi)^2}$) of 0.0025 (the smallest value for which no significant contamination is observed) around the direction of a muon from the Z boson decay. The MC gives a good description of the resulting invariant mass distributions for reconstructed Z bosons [40].

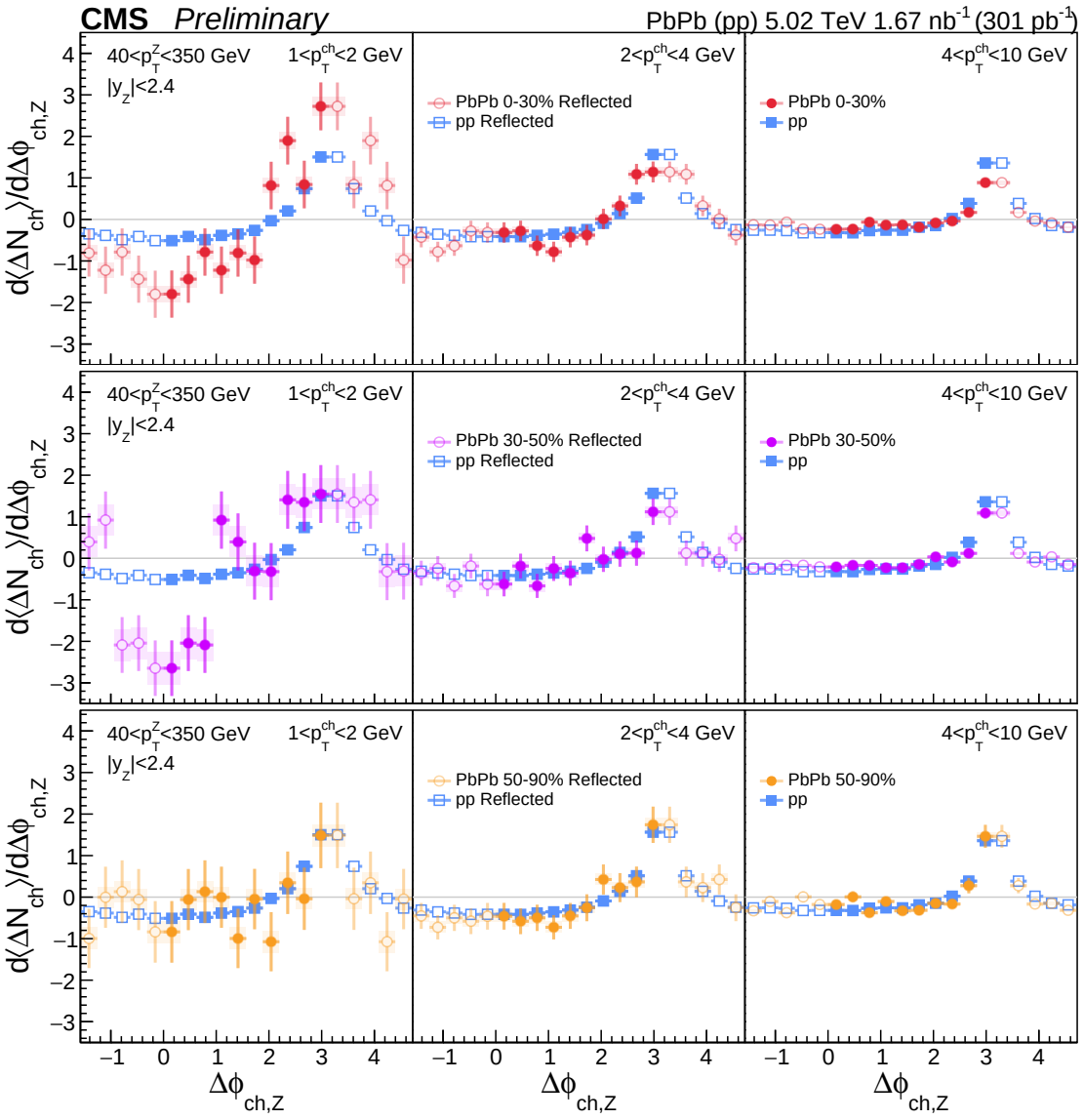

Figure 1: The $\Delta\phi_{\mathrm{ch,Z}}$ spectra in the Z boson side for events with Z boson $p_{\mathrm{T}}^{\mathrm{Z}} > 40$ GeV in pp and PbPb collisions. The filled circles (squares) are the PbPb (pp) data and the open circles (squares) are reflected data. The vertical bars and shaded boxes represent the statistical and systematic uncertainties, respectively. The results are presented in centrality intervals of 0–30%, 30–50%, and 50-90% and in the charged hadron $p_{\mathrm{T}}^{\mathrm{ch}}$ intervals of 1–2 (left), 2–4 and 4–10 GeV (right).

To focus on charged hadrons associated with the Z boson and reveal possible medium-induced modifications, an event-mixing scheme is employed to subtract the substantial background from multi-parton interactions in heavy-ion collisions. The charged hadron spectrum is divided into the shape component ΔN_{ch} (normalized associated yield, where $\mathrm{N_{ch}}$ is the number of associated charged hadrons), which integrates to zero, and the normalization component $\langle N_{\mathrm{ch}} \rangle$. This results in the expression of normalized associated yield:

$$\frac{1}{\mathrm{N_Z}} \Delta\langle \mathrm{N_{ch}} \rangle (\Delta\phi_{\mathrm{ch,Z}}, \Delta y_{\mathrm{ch,Z}}) = \frac{\mathrm{N_{ch}}(\Delta\phi_{\mathrm{ch,Z}}, \Delta y_{\mathrm{ch,Z}}) - \langle \mathrm{N_{ch}} \rangle}{\mathrm{N_Z}}, \tag{1}$$

where N_Z is the number of leading Z boson, and $\langle \mathrm{N_{ch}} \rangle$ is the average over the distribution. The $\Delta\langle \mathrm{N_{ch}} \rangle$ is extracted using a mixed-event subtraction method by correlating the Z boson from each Z boson event with the charged hadrons from another Z boson event within the sample, repeated for 10 other events to reduce statistical fluctuations. Let $S(\Delta\phi_{\mathrm{ch,Z}}, \Delta y_{\mathrm{ch,Z}})$ represent the same-event correlation function and $B(\Delta\phi_{\mathrm{ch,Z}}, \Delta y_{\mathrm{ch,Z}})$ represent the mixed-event correlation function. The relationship between $\Delta \mathrm{N_{ch}}$ and these functions can be written as:

$$\frac{1}{\mathrm{N_Z}} \Delta\langle \mathrm{N_{ch}} \rangle (\Delta\phi_{\mathrm{ch,Z}}, \Delta y_{\mathrm{ch,Z}}) = S(\Delta\phi_{\mathrm{ch,Z}}, \Delta y_{\mathrm{ch,Z}}) - B(\Delta\phi_{\mathrm{ch,Z}}, \Delta y_{\mathrm{ch,Z}}) \tag{2}$$

This method subtracts the UE and $\langle \mathrm{N_{ch}} \rangle$ contributions, isolating the medium-induced modifications. In this analysis, results for positive and negative $\Delta\phi_{\mathrm{ch,Z}}$ ($\Delta y_{\mathrm{ch,Z}}$) are merged to improve statistical precision. The merged results, taken from measurements with respect to $|\Delta\phi_{\mathrm{ch,Z}}|$ ($|\Delta y_{\mathrm{ch,Z}}|$), are then scaled by a factor of 0.5 in order to ensure that the total integrated yield accurately reflects the relative excess or depletion observed in the data and allows for direct comparison with theoretical predictions. In order to make a clearer visual presentation of the data, the results are "reflected", i.e. the same values are plotted at both positive and negative $\Delta y_{\mathrm{ch,Z}}$, while for $\Delta\phi_{\mathrm{ch,Z}}$, data points are reflected around both 0 and π.

Several variations in the analysis are considered to account for uncertainties related to tracking efficiency and corrections, muon identification and reconstruction efficiency, as well as pp pileup and PbPb background subtraction. Systematic uncertainties are evaluated as the differences between final results and those obtained with varied settings.

The uncertainty related to tracking efficiency is estimated by comparing track reconstruction efficiency between data and simulation [16]. An efficiency uncertainty of 5% (2.4%) per charged hadron track was quoted as the systematic uncertainty in the PbPb (pp) analysis. Muon efficiencies are varied according to the uncertainty in their data-to-MC differences, obtained using the "tag-and-probe" method [54]. For systematic uncertainties associated with pileup in pp collisions, the nominal distributions are compared to those from events without a single primary vertex requirement. The centrality calibration is varied to calculate the effect of the minimum bias event selection efficiency of the HF calorimeters [39]. The uncertainties are then summed in quadrature to obtain the final systematic uncertainties and are significantly smaller than the statistical uncertainty. When calculating the systematics of the difference between pp and PbPb spectra, we assume the systematics are uncorrelated and sum them in quadrature.

The distributions of the azimuthal angle difference, $\Delta\phi_{\mathrm{ch,Z}}$, between the Z boson and charged hadron tracks in three charged hadron $p_{\mathrm{T}}^{\mathrm{ch}}$ intervals are shown in Fig. 1. In pp collisions, the distribution features an away-side peak at $\Delta\phi_{\mathrm{ch,Z}} \sim \pi$, while on the near-side close to the Z

boson, the normalized associated yield is flat and becomes negative. To investigate the centrality dependence of the medium-induced modification, the results from PbPb data are studied in three centrality classes: 0–30%, 30–50%, and 50–90%. The fully corrected PbPb data are then compared to the reference pp data.

In the 0–30% centrality class, significant modifications are observed in the zero-area normalized distributions compared to the pp reference in the highest and lowest p_{T} intervals. A larger modulation $\Delta\phi_{\mathrm{ch,Z}}$ distribution is observed for low-p_{T} tracks within the $1 < p_{\mathrm{T}} < 2$ GeV range, aligning with the expected response from parton-medium interactions. For the intermediate p_{T} range of 2–4 GeV, the PbPb data resemble the pp reference more closely than the lowest p_{T} charged hadrons. Significant suppression of high-p_{T} particles is observed on the away-side (jet region) for high charged hadron p_{T} within the 4–10 GeV range, especially when $|\Delta\phi_{\mathrm{ch,Z}}| > \pi/2$. The difference between the PbPb and pp data diminishes at high charged hadron p_{T} as we move towards more peripheral collisions. The pp data and the PbPb data at 50–90% are consistent with each other.

The spectra of the pseudorapidity difference between the charged hadron and the Z boson, $\Delta y_{\mathrm{ch,Z}}$, are presented in Fig. 2. Note that the area of the spectra shown in these figures is not expected to be zero due to the additional $\Delta\phi_{\mathrm{ch,Z}}$ requirement. On the Z boson side, the observable $\Delta y_{\mathrm{ch,Z}}$ is sensitive to the medium-recoil effect, which would appear as a dip structure at $\Delta y_{\mathrm{ch,Z}} \sim 0$. As shown in Fig. 2, the normalized associated yield measured from pp data on the Z boson side is smaller than zero. The same measurement is also performed with PbPb data. At low p_{T}, the PbPb data are significantly below the pp reference. This difference diminishes in the 2 to 4 GeV range. At high p_{T}, the PbPb data are higher than the pp reference. In the most peripheral PbPb collisions (50–90%), the difference between pp and PbPb data disappears.

In order to gain deeper insights into the results, the PbPb data are also compared to jet quenching models. The "Pythia Quenched" (PYQUEN 1.5.3) model approximates radiative and collisional energy loss mechanisms phenomenologically without strict enforcement of local energy-momentum conservation. The model can be used to predict the shower of high-energy partons traversing the QGP, resulting in medium-induced modifications to jet structures and particle correlations. The model predicts that the Z-hadron correlation is influenced by collisions and radiative effects induced by the medium, leading to substantial changes in the jet fragmentation function. The "Jet Evolution With Energy Loss" (JEWEL 2.2.0) model simulates the interaction of jets with a QGP with pQCD-based calculations, incorporating both radiative and collisional energy losses. It predicts jet modifications due to the medium, including the recoil of medium particles. The model can be run in two modes: with recoil, conserving energy and momentum, and without recoil, which does not conserve energy and momentum but enables a focus on the quenched parton shower. According to this model, medium recoils significantly enhance the low p_{T} normalized associated yield on the jet side, while medium holes around the Z boson reduce the normalized associated yield [55, 56]. Medium holes are regions in the QGP depleted of energy and momentum due to the jet-medium scattering, leading to a suppression of particle production in these areas. In JEWEL 2.2.0, the recoil parton and holes do not rescatter. The "Hybrid model" (HYBRID), based on AdS/CFT correspondence, combines perturbative QCD calculations with strong coupling dynamics to simulate jet interactions within the QGP [24]. This approach provides a comprehensive framework for understanding the energy loss and modifications of jets traversing the QGP. The positive wake associated with the jet shower enhances the jet-side normalized associated yield, while the negative wake on the Z-side suppresses the normalized associated yield around the Z bosons [57]. Finally, the Coupled Linear Boltzmann Transport model (CO-LBT) combines the Linear Boltzmann Transport equation, which governs parton energy loss through scattering and radiation in the QGP, with

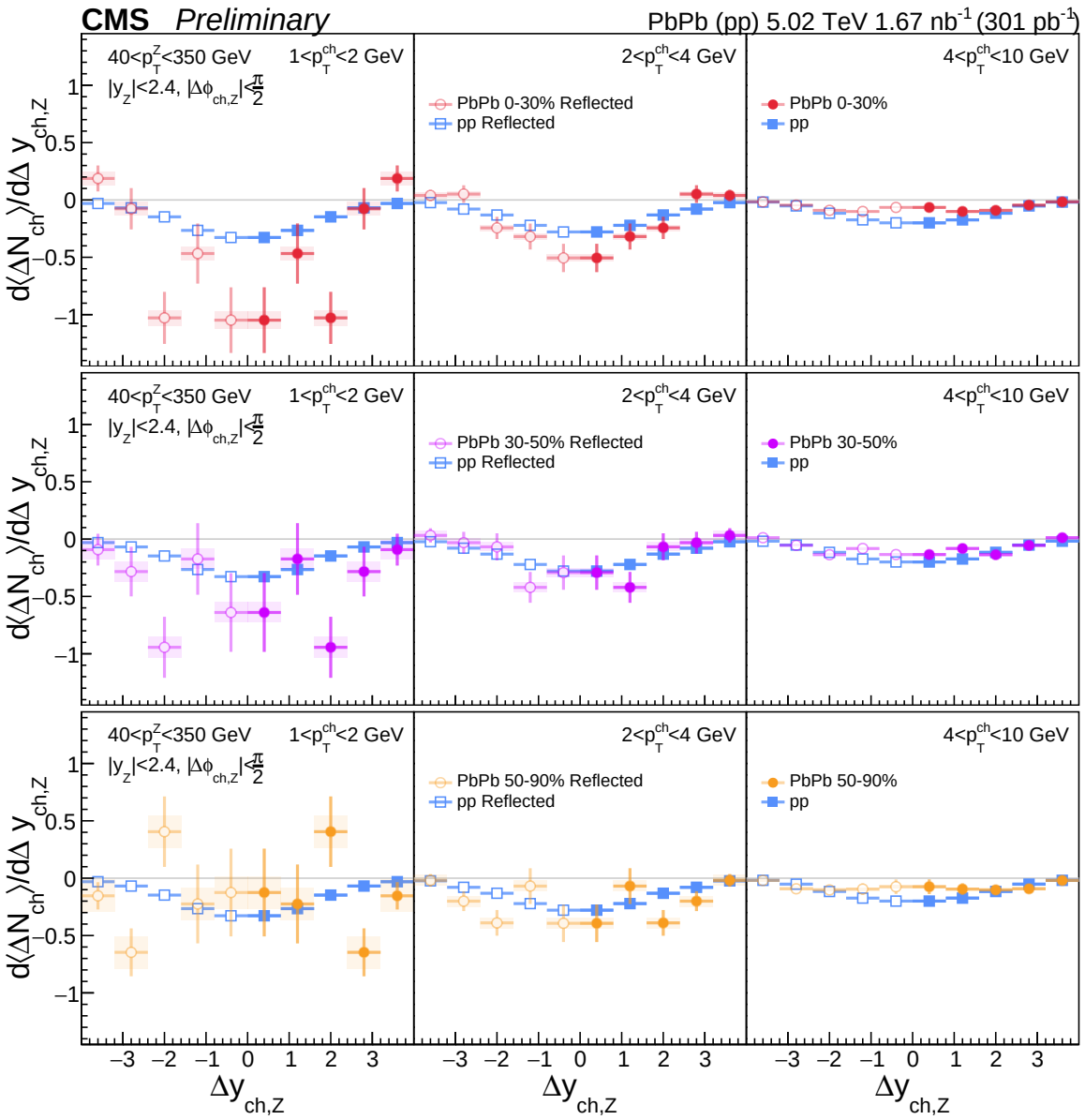

Figure 2: The $\Delta y_{\mathrm{ch,Z}}$ spectra in the Z boson side ($|\Delta\phi_{\mathrm{ch,Z}}| < \pi/2$) for events with Z boson $p_{\mathrm{T}}^{\mathrm{Z}} > 40\,\mathrm{GeV}$ in pp and PbPb collisions. The filled circles (squares) are the PbPb (pp) data and the open circles (squares) are reflected data. The vertical bars and shaded boxes represent the statistical and systematic uncertainties, respectively. The results are presented in centrality intervals of 0–30%, 30–50%, and 50-90% and in the charged hadron $p_{\mathrm{T}}^{\mathrm{ch}}$ intervals of 1–2 (left), 2–4 and 4–10 GeV (right).

hydrodynamic simulations that describe the bulk evolution of the QGP [58]. At low charged-hadron p_{T}, the reheating of the QGP due to quenched energy is linked to the enhanced yield on the jet side of the normalized associated yield, while the diffusion wake, the diffusion of the "particle holes" behind the hard-scattered parton, results in the suppression of the normalized associated yield on the Z boson side [41, 42].

Figures 3 and 4 show the comparison between the 0–30% PbPb data and theoretical predictions. The full HYBRID model, which includes both negative and positive wake contributions, displays a dip structure at small $\Delta\phi_{\mathrm{ch,Z}}$ and $\Delta y_{\mathrm{ch,Z}}$ due to the negative wake, and an excess at $\Delta\phi_{\mathrm{ch,Z}} \sim \pi$ due to the positive wake. This model provides a good description of the central PbPb data. However, excluding the wake contribution, the HYBRID model fails to describe the data accurately. The JEWEL model explains the dip structure at $\Delta\phi_{\mathrm{ch,Z}} = \pi$ as resulting from medium recoils, emphasizing their impact on the azimuthal distribution. Additionally, the dip in $\Delta y_{\mathrm{ch,Z}}$ is also linked to medium recoils, with the model predicting a narrower dip due to the absence of parton rescattering in this version. Without medium recoils, JEWEL also fails to describe the data accurately. The PYQUEN model predicts smaller modifications of the Z-tagged charged hadron spectra and fails to describe the dip structure at small $\Delta\phi_{\mathrm{ch,Z}}$ and $\Delta y_{\mathrm{ch,Z}}$ due to a lack of energy-momentum conservation. The CO-LBT model provides a reasonable description of the $\Delta\phi_{\mathrm{ch,Z}}$ spectra in three different ranges of charged-hadron p_{T}. However, the model predicts a larger (i.e. less negative) normalized associated yield at small $\Delta y_{\mathrm{ch,Z}}$ compared to the data in the charged-hadron p_{T} range between 1 and 4 GeV. Finally, the PbPb data are compared to PYTHIA 8 events with a lower $p_{\mathrm{T}}^{\mathrm{Z}}$ selection, where the $p_{\mathrm{T}}^{\mathrm{Z}}$ threshold of 20 GeV is selected to roughly match the high $p_{\mathrm{T}}^{\mathrm{ch}}$ normalized associated yield distribution. This comparison is intended to emulate the effect of jet quenching by seeing if a quenched jet in PbPb collisions resembles a lower-p_{T} vacuum jet. However, the PbPb data diverge from the low $p_{\mathrm{T}}^{\mathrm{Z}}$ events at low $p_{\mathrm{T}}^{\mathrm{ch}}$, indicating that the quenched jets are not simply a shift to lower p_{T} vacuum-like jets.

Based on the data-to-model comparison, PbPb data are better reproduced by theoretical models that include medium recoil effects. Moreover, the PbPb data differ from lower $p_{\mathrm{T}}^{\mathrm{Z}}$ Z-tagged events. These results provide the first evidence of the medium recoil and hole effects around the Z boson. However, it remains unclear which theoretical model of medium recoil effect best agrees with the data.

In summary, this note presents the first measurement of Z-tagged charged hadron spectra in bins of charged hadron p_{T} in pp and PbPb collisions at $\sqrt{s_{\mathrm{NN}}} = 5.02$ TeV. The spectra are analyzed with respect to the Z boson, specifically in pseudorapidity distribution and azimuthal angle, for Z bosons within the $40 < p_{\mathrm{T}}^{\mathrm{Z}} < 350$ GeV range. The analysis utilizes data from 2017 and 2018, with integrated luminosities of 301 ± 6 pb^{-1} and 1.67 ± 0.03 nb^{-1}, respectively.

The normalized associated yield of Z-tagged charged hadrons in bins of azimuthal angle difference ($\Delta\phi_{\mathrm{ch,Z}}$) and rapidity difference ($\Delta y_{\mathrm{ch,Z}}$) are compared between the PbPb and reference pp data. In PbPb collisions, a dip at $\Delta\phi_{\mathrm{ch,Z}} = 0$ indicates negative medium wake or medium holes, and an excess at $\Delta\phi_{\mathrm{ch,Z}} = \pi$ suggests medium-induced radiation and momentum-broadening effects. Central collisions show a larger modulation in $\Delta\phi_{\mathrm{ch,Z}}$ distribution at low p_{T} than pp data, and the difference diminishes in more peripheral events. At high p_{T} ($4 < p_{\mathrm{T}} < 10$ GeV), a reduction in the jet peak normalized associated yield is consistent with the expectation from jet quenching. The $\Delta y_{\mathrm{ch,Z}}$ distribution shows significant deviations in central collisions with respect to the pp reference, especially at low charged hadron p_{T}, where the PbPb yield is lower than pp near the Z boson ($|\Delta y_{\mathrm{ch,Z}}| \sim 0$).

The full HYBRID model, incorporating both negative and positive wake contributions, gives a good description of the central PbPb data, showing a dip at small $\Delta\phi_{\mathrm{ch,Z}}$ and $\Delta y_{\mathrm{ch,Z}}$ due to the

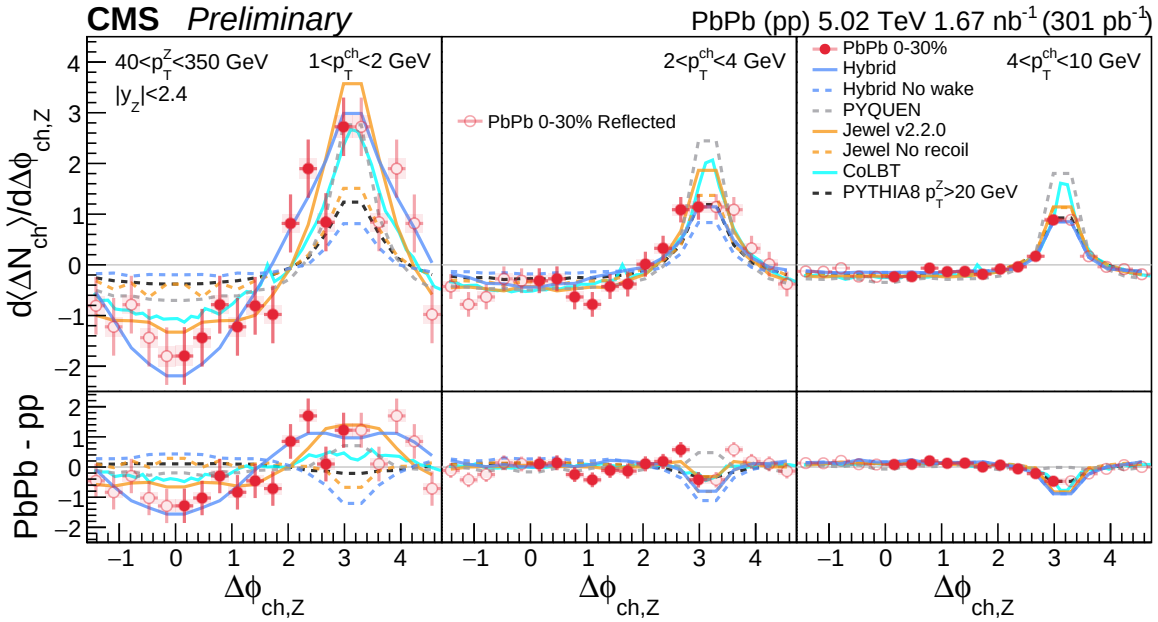

Figure 3: Upper: Distributions of $\Delta\phi_{\mathrm{ch,Z}}$ in pp collisions compared to 0–30% PbPb collisions (left to right) in the charged hadron $p_{\mathrm{T}}^{\mathrm{ch}}$ intervals of 1–2 (left), 2–4 and 4–10 GeV (right). Lower: Difference between the PbPb and pp distributions. The filled circles are PbPb data and the open circles are reflected data. The vertical bars and shaded boxes represent the statistical and systematic uncertainties, respectively. The results are compared to predictions from theoretical models.

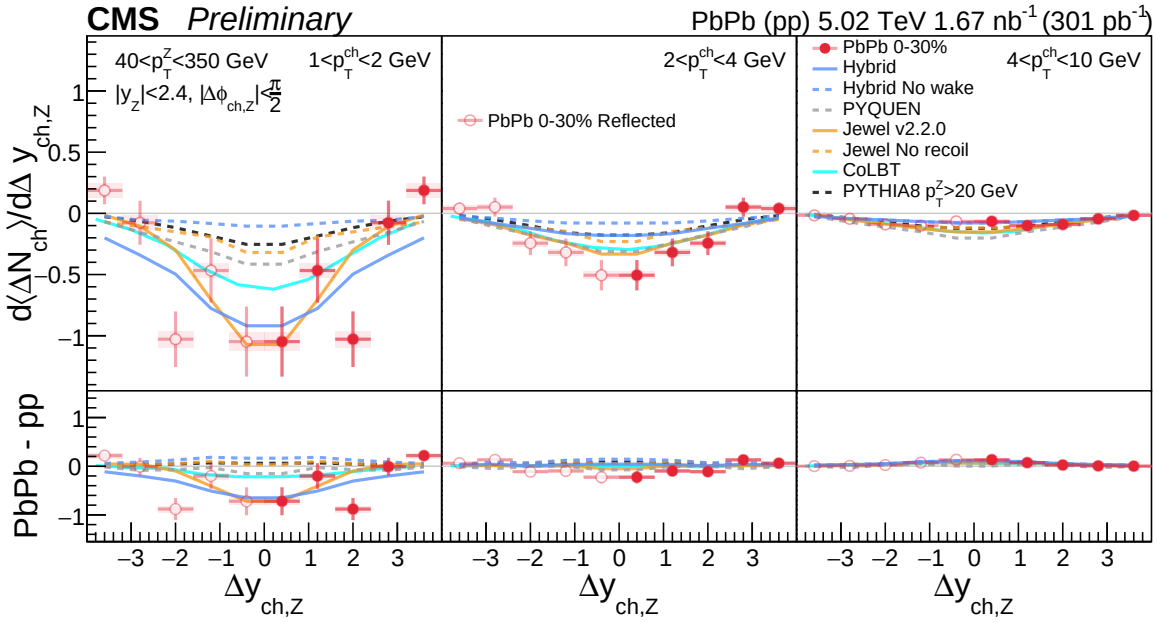

Figure 4: Upper: Distributions of $\Delta y_{\mathrm{ch,Z}}$ in pp collisions compared to 0–30% PbPb collisions (left to right) in the charged hadron $p_{\mathrm{T}}^{\mathrm{ch}}$ intervals of 1–2 (left), 2–4 and 4–10 GeV (right). Lower: Difference between the PbPb and pp distributions. The filled circles are PbPb data and the open circles are reflected data. The vertical bars and shaded boxes represent the statistical and systematic uncertainties, respectively. The results are compared to predictions from theoretical models.

negative wake, and excess at $\Delta\phi_{\mathrm{ch,Z}} \sim \pi$ due to the positive wake. The JEWEL model attributes the dip to negative contributions from holes and the excess at $\Delta\phi_{\mathrm{ch,Z}} = \pi$ to medium recoils, predicting a narrower $\Delta y_{\mathrm{ch,Z}}$ dip due to the absence of parton rescattering. Without a medium response, both HYBRID and JEWEL models fail to represent the data accurately. The PYQUEN model, which lacks energy-momentum conservation, predicts smaller modifications than the ones observed in data and fails to capture the dip structure at small $\Delta\phi_{\mathrm{ch,Z}}$ and $\Delta y_{\mathrm{ch,Z}}$ values. The CO-LBT model predicts an enhancement of normalized associated yield on the jet side due to reheating of the QGP caused by quenched energy, while the diffusion wakes trailing the hard-scattered parton suppresses the normalized associated yield on the Z boson side. This model provides a reasonable description of the $\Delta\phi_{\mathrm{ch,Z}}$ spectra but overestimates the normalized associated yield at small $\Delta y_{\mathrm{ch,Z}}$ for low charged-hadron p_{T}. Finally, PbPb data are compared to PYTHIA 8 events with a $p_{\mathrm{T}}^{\mathrm{Z}}$ threshold of 20 GeV, tuned to match the high $p_{\mathrm{T}}^{\mathrm{ch}}$ normalized associated yield distribution, to see if a quenched jet in data resembles a lower-energy vacuum jet. However, the PbPb data diverge from PYTHIA 8 at low $p_{\mathrm{T}}^{\mathrm{ch}}$, indicating that quenched jets are not merely lower p_{T} vacuum-like jets.

The PbPb data are better reproduced by theoretical models that include medium recoil effects and differ from lower $p_{\mathrm{T}}^{\mathrm{Z}}$ Z-tagged events. The data provide significant new inputs on jet quenching models and the correlation between hard and soft particles in heavy-ion collisions. These findings provide the first evidence of medium recoil and hole effects caused by a hard probe, though it remains unclear which theoretical model on the medium recoils and negative wake best aligns with the data.

References

[1] J. C. Collins and M. J. Perry, "Superdense matter: Neutrons or asymptotically free quarks?", *Phys. Rev. Lett.* **34** (1975) 1353, doi:10.1103/PhysRevLett.34.1353.

[2] F. Karsch, "The phase transition to the quark gluon plasma: recent results from lattice calculations", *Nucl. Phys. A* **590** (1995) 367, doi:10.1016/0375-9474(95)00248-Y, arXiv:hep-lat/9503010.

[3] W. Busza, K. Rajagopal, and W. van der Schee, "Heavy Ion Collisions: The Big Picture, and the Big Questions", *Ann. Rev. Nucl. Part. Sci.* **68** (2018) 339, doi:10.1146/annurev-nucl-101917-020852, arXiv:1802.04801.

[4] STAR Collaboration, "Experimental and theoretical challenges in the search for the quark gluon plasma: The STAR Collaboration's critical assessment of the evidence from RHIC collisions", *Nucl. Phys. A* **757** (2005) 102, doi:10.1016/j.nuclphysa.2005.03.085, arXiv:nucl-ex/0501009.

[5] PHENIX Collaboration, "Formation of dense partonic matter in relativistic nucleus-nucleus collisions at RHIC: Experimental evaluation by the PHENIX collaboration", *Nucl. Phys. A* **757** (2005) 184, doi:10.1016/j.nuclphysa.2005.03.086, arXiv:nucl-ex/0410003.

[6] PHOBOS Collaboration, "The PHOBOS perspective on discoveries at RHIC", *Nucl. Phys. A* **757** (2005) 28, doi:10.1016/j.nuclphysa.2005.03.084, arXiv:nucl-ex/0410022.

[7] BRAHMS Collaboration, "Quark gluon plasma and color glass condensate at RHIC? The Perspective from the BRAHMS experiment", *Nucl. Phys. A* **757** (2005) 1, doi:10.1016/j.nuclphysa.2005.02.130, arXiv:nucl-ex/0410020.

[8] ALICE Collaboration, "The ALICE experiment – A journey through QCD", arXiv:2211.04384.

[9] CMS Collaboration, "Overview of high-density QCD studies with the CMS experiment at the LHC", arXiv:2405.10785.

[10] J. D. Bjorken, "Highly relativistic nucleus-nucleus collisions: The central rapidity region", *Phys. Rev. D* **27** (1983) 140, doi:10.1103/PhysRevD.27.140.

[11] STAR Collaboration, "Transverse-momentum and collision-energy dependence of high-p_{t} hadron suppression in Au+Au collisions at ultrarelativistic energies", *Phys. Rev. Lett.* **91** (2003) 172302, doi:10.1103/PhysRevLett.91.172302, arXiv:nucl-ex/0305015.

[12] PHENIX Collaboration, "Suppression pattern of neutral pions at high transverse momentum in Au+Au collisions at $\sqrt{s_{\mathrm{NN}}} = 200$ GeV and constraints on medium transport coefficients", *Phys. Rev. Lett.* **101** (2008) 232301, doi:10.1103/PhysRevLett.101.232301, arXiv:0801.4020.

[13] ALICE Collaboration, "Centrality dependence of charged particle production at large transverse momentum in Pb–Pb collisions at $\sqrt{s_{\mathrm{NN}}} = 2.76$ TeV", *Phys. Lett. B* **720** (2013) 52, doi:10.1016/j.physletb.2013.01.051, arXiv:1208.2711.

[14] ATLAS Collaboration, "Measurement of charged-particle spectra in Pb+Pb collisions at $\sqrt{s_{\mathrm{NN}}} = 2.76$ TeV with the ATLAS detector at the LHC", *JHEP* **09** (2015) 050, doi:10.1007/JHEP09(2015)050, arXiv:1504.04337.

[15] CMS Collaboration, "Study of high-p_{T} charged particle suppression in PbPb compared to pp collisions at $\sqrt{s_{\mathrm{NN}}} = 2.76$ TeV", *Eur. Phys. J. C* **72** (2012) 1945, doi:10.1140/epjc/s10052-012-1945-x, arXiv:1202.2554.

[16] CMS Collaboration, "Charged-particle nuclear modification factors in PbPb and pPb collisions at $\sqrt{s_{\mathrm{NN}}} = 5.02$ TeV", *JHEP* **04** (2017) 039, doi:10.1007/JHEP04(2017)039, arXiv:1611.01664.

[17] CMS Collaboration, "Observation and studies of jet quenching in PbPb collisions at $\sqrt{s_{\mathrm{NN}}} = 2.76$ TeV", *Phys. Rev. C* **84** (2011) 024906, doi:10.1103/PhysRevC.84.024906, arXiv:1102.1957.

[18] ATLAS Collaboration, "Observation of a centrality-dependent dijet asymmetry in lead-lead collisions at $\sqrt{s_{\mathrm{NN}}} = 2.76$ TeV with the ATLAS detector at the LHC", *Phys. Rev. Lett.* **105** (2010) 252303, doi:10.1103/PhysRevLett.105.252303, arXiv:1011.6182.

[19] ATLAS Collaboration, "Centrality and rapidity dependence of inclusive jet production in $\sqrt{s_{\mathrm{NN}}} = 5.02$ TeV proton–lead collisions with the ATLAS detector", *Phys. Lett. B* **748** (2015) 392, doi:10.1016/j.physletb.2015.07.023, arXiv:1412.4092.

[20] ALICE Collaboration, "Measurement of jet quenching with semi-inclusive hadron-jet distributions in central Pb-Pb collisions at $\sqrt{s_{\mathrm{NN}}} = 2.76$ TeV", *JHEP* **09** (2015) 170, doi:10.1007/JHEP09(2015)170, arXiv:1506.03984.

[21] CMS Collaboration, "Measurement of inclusive jet cross sections in pp and PbPb collisions at $\sqrt{s_{\mathrm{NN}}} = 2.76\,\mathrm{TeV}$", *Phys. Rev. C* **96** (2017) 015202, doi:10.1103/PhysRevC.96.015202, arXiv:1609.05383.

[22] ALICE Collaboration, "Measurement of jet suppression in central Pb-Pb collisions at $\sqrt{s_{\mathrm{NN}}} = 2.76\,\mathrm{TeV}$", *Phys. Lett. B* **746** (2015) 1, doi:10.1016/j.physletb.2015.04.039, arXiv:1502.01689.

[23] STAR Collaboration, "Dijet imbalance measurements in Au+Au and pp collisions at $\sqrt{s_{\mathrm{NN}}} = 200\,\mathrm{GeV}$ at STAR", *Phys. Rev. Lett.* **119** (2017) 062301, doi:10.1103/PhysRevLett.119.062301, arXiv:1609.03878.

[24] J. Casalderrey-Solana et al., "A Hybrid Strong/Weak Coupling Approach to Jet Quenching", *JHEP* **10** (2014) 019, doi:10.1007/JHEP10(2014)019, arXiv:1405.3864.

[25] L. Apolinário, Y.-J. Lee, and M. Winn, "Heavy quarks and jets as probes of the QGP", *Prog. Part. Nucl. Phys.* **127** (2022) 103990, doi:10.1016/j.ppnp.2022.103990, arXiv:2203.16352.

[26] S. Cao and G.-Y. Qin, "Medium Response and Jet–Hadron Correlations in Relativistic Heavy-Ion Collisions", *Ann. Rev. Nucl. Part. Sci.* **73** (2023) 205, doi:10.1146/annurev-nucl-112822-031317, arXiv:2211.16821.

[27] ATLAS Collaboration, "Centrality, rapidity and transverse momentum dependence of isolated prompt photon production in lead-lead collisions at $\sqrt{s_{\mathrm{NN}}} = 2.76\,\mathrm{TeV}$ measured with the ATLAS detector", *Phys. Rev. C* **93** (2016) 034914, doi:10.1103/PhysRevC.93.034914, arXiv:1506.08552.

[28] CMS Collaboration, "Measurement of isolated photon production in pp and PbPb collisions at $\sqrt{s_{\mathrm{NN}}} = 2.76\,\mathrm{TeV}$", *Phys. Lett. B* **710** (2012) 256, doi:10.1016/j.physletb.2012.02.077, arXiv:1201.3093.

[29] CMS Collaboration, "Study of W boson production in PbPb and pp collisions at $\sqrt{s_{\mathrm{NN}}} = 2.76\,\mathrm{TeV}$", *Phys. Lett. B* **715** (2012) 66, doi:10.1016/j.physletb.2012.07.025, arXiv:1205.6334.

[30] CMS Collaboration, "Study of Z production in PbPb and pp collisions at $\sqrt{s_{\mathrm{NN}}} = 2.76\,\mathrm{TeV}$ in the dimuon and dielectron decay channels", *JHEP* **03** (2015) 022, doi:10.1007/JHEP03(2015)022, arXiv:1410.4825.

[31] CMS Collaboration, "The production of isolated photons in PbPb and pp collisions at $\sqrt{s_{\mathrm{NN}}} = 5.02\,\mathrm{TeV}$", *JHEP* **07** (2020) 116, doi:10.1007/JHEP07(2020)116, arXiv:2003.12797.

[32] V. Kartvelishvili, R. Kvatadze, and R. Shanidze, "On Z and Z+jet production in heavy ion collisions", *Phys. Lett. B* **356** (1995) 589, doi:10.1016/0370-2693(95)00865-I, arXiv:hep-ph/9505418.

[33] X.-N. Wang, Z. Huang, and I. Sarcevic, "Jet quenching in the opposite direction of a tagged photon in high-energy heavy ion collisions", *Phys. Rev. Lett.* **77** (1996) 231, doi:10.1103/PhysRevLett.77.231, arXiv:hep-ph/9605213.

[34] X.-N. Wang and Z. Huang, "Medium-induced parton energy loss in γ+jet events of high-energy heavy-ion collisions", *Phys. Rev. C* **55** (1997) 3047, doi:10.1103/PhysRevC.55.3047, arXiv:hep-ph/9701227.

[35] J. Brewer, Q. Brodsky, and K. Rajagopal, "Disentangling jet modification in jet simulations and in Z+jet data", *JHEP* **02** (2022) 175, doi:10.1007/JHEP02(2022)175, arXiv:2110.13159.

[36] W. Dai, I. Vitev, and B.-W. Zhang, "Momentum imbalance of isolated photon-tagged jet production at RHIC and LHC", *Phys. Rev. Lett.* **110** (2013) 142001, doi:10.1103/PhysRevLett.110.142001, arXiv:1207.5177.

[37] Z.-B. Kang, I. Vitev, and H. Xing, "Vector-boson-tagged jet production in heavy ion collisions at energies available at the CERN large hadron collider", *Phys. Rev. C* **96** (2017) 014912, doi:10.1103/PhysRevC.96.014912, arXiv:1702.07276.

[38] CMS Collaboration, "Study of Jet Quenching with $Z+$jet Correlations in Pb-Pb and pp Collisions at $\sqrt{s_{NN}} = 5.02$ TeV", *Phys. Rev. Lett.* **119** (2017), no. 8, 082301, doi:10.1103/PhysRevLett.119.082301, arXiv:1702.01060.

[39] CMS Collaboration, "Constraints on the Initial State of Pb-Pb Collisions via Measurements of Z-Boson Yields and Azimuthal Anisotropy at $\sqrt{s_{NN}}$=5.02 TeV", *Phys. Rev. Lett.* **127** (2021), no. 10, 102002, doi:10.1103/PhysRevLett.127.102002, arXiv:2103.14089.

[40] CMS Collaboration, "Using Z Boson Events to Study Parton-Medium Interactions in Pb-Pb Collisions", *Phys. Rev. Lett.* **128** (2022), no. 12, 122301, doi:10.1103/PhysRevLett.128.122301, arXiv:2103.04377.

[41] Z. Yang et al., "Search for the Elusive Jet-Induced Diffusion Wake in Z/γ-Jets with 2D Jet Tomography in High-Energy Heavy-Ion Collisions", *Phys. Rev. Lett.* **127** (2021), no. 8, 082301, doi:10.1103/PhysRevLett.127.082301, arXiv:2101.05422.

[42] Z. Yang et al., "3D Structure of Jet-Induced Diffusion Wake in an Expanding Quark-Gluon Plasma", *Phys. Rev. Lett.* **130** (2023), no. 5, 052301, doi:10.1103/PhysRevLett.130.052301, arXiv:2203.03683.

[43] F. D'Eramo, M. Lekaveckas, H. Liu, and K. Rajagopal, "Momentum Broadening in Weakly Coupled Quark-Gluon Plasma (with a view to finding the quasiparticles within liquid quark-gluon plasma)", *JHEP* **05** (2013) 031, doi:10.1007/JHEP05(2013)031, arXiv:1211.1922.

[44] Y. He, T. Luo, X.-N. Wang, and Y. Zhu, "Linear Boltzmann Transport for Jet Propagation in the Quark-Gluon Plasma: Elastic Processes and Medium Recoil", *Phys. Rev. C* **91** (2015) 054908, doi:10.1103/PhysRevC.91.054908, arXiv:1503.03313. [Erratum: Phys.Rev.C 97, 019902 (2018)].

[45] CMS Collaboration, "The CMS experiment at the CERN LHC", *JINST* **3** (2008) S08004, doi:10.1088/1748-0221/3/08/S08004.

[46] CMS Collaboration, "The CMS trigger system", *JINST* **12** (2017) P01020, doi:10.1088/1748-0221/12/01/P01020, arXiv:1609.02366.

[47] T. Sjöstrand et al., "An Introduction to PYTHIA 8.2", *Comput. Phys. Commun.* **191** (2015) 159, doi:10.1016/j.cpc.2015.01.024, arXiv:1410.3012.

[48] CMS Collaboration, "Extraction and validation of a new set of CMS PYTHIA8 tunes from underlying-event measurements", arXiv:1903.12179.

[49] J. Alwall et al., "The automated computation of tree-level and next-to-leading order differential cross sections, and their matching to parton shower simulations", *JHEP* **07** (2014) 079, doi:10.1007/JHEP07(2014)079, arXiv:1405.0301.

[50] I. P. Lokhtin and A. M. Snigirev, "A model of jet quenching in ultrarelativistic heavy ion collisions and high-p_{T} hadron spectra at RHIC", *Eur. Phys. J. C* **45** (2006) 211, doi:10.1140/epjc/s2005-02426-3, arXiv:hep-ph/0506189.

[51] GEANT4 Collaboration, "GEANT4—a simulation toolkit", *Nucl. Instrum. Meth. A* **506** (2003) 250, doi:10.1016/S0168-9002(03)01368-8.

[52] CMS Collaboration, "Performance of CMS muon reconstruction in pp collision events at $\sqrt{s} = 7$ TeV", *JINST* **7** (2012) P10002, doi:10.1088/1748-0221/7/10/P10002, arXiv:1206.4071.

[53] CMS Collaboration, "Description and performance of track and primary-vertex reconstruction with the CMS tracker", *JINST* **9** (2014) P10009, doi:10.1088/1748-0221/9/10/P10009, arXiv:1405.6569.

[54] C. Collaboration, "Measurements of inclusive w and z cross sections in pp collisions at sqrt(s)=7 tev", *JHEP* **10** (2011) 132, doi:10.1007/JHEP10(2011)132, arXiv:1107.4789.

[55] K. C. Zapp, "JEWEL 2.0.0: directions for use", *Eur. Phys. J. C* **74** (2014), no. 2, 2762, doi:10.1140/epjc/s10052-014-2762-1, arXiv:1311.0048.

[56] R. Kunnawalkam Elayavalli and K. C. Zapp, "Medium response in JEWEL and its impact on jet shape observables in heavy ion collisions", *JHEP* **07** (2017) 141, doi:10.1007/JHEP07(2017)141, arXiv:1707.01539.

[57] J. Casalderrey-Solana et al., "Jet Wake from Linearized Hydrodynamics", *JHEP* **05** (2021) 230, doi:10.1007/JHEP05(2021)230, arXiv:2010.01140.

[58] W. Chen et al., "Effects of jet-induced medium excitation in γ-hadron correlation in A+A collisions", *Phys. Lett. B* **777** (2018) 86, doi:10.1016/j.physletb.2017.12.015, arXiv:1704.03648.